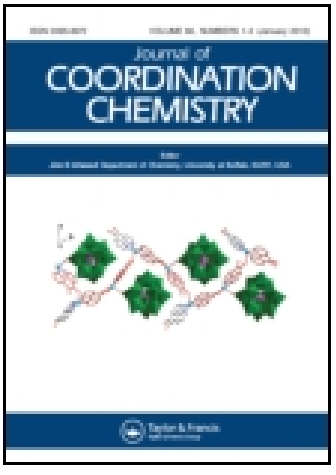

Journal of Coordination Chemistry
Publication details, including instructions for authors and subscription information:
http://www.tandfonline.com/loi/gcoo20

Synthesis, characterization, spectrophotometric investigation, structural study, and antibacterial activities of a series of new zinc(II) complexes

Azam Zamani[a], Mehdi Salehi[a], S. Maryam Sajjadi[a], Maciej Kubicki[b], Grzegorz Dutkiewicz[b] & Ali Khaleghian[c]

[a] Department of Chemistry, College of Science, Semnan University, Semnan, Iran

[b] Faculty of Chemistry, Adam Mickiewicz University, Poznan, Poland

[c] Department of Biochemistry, Semnan University of Medical Science, Semnan, Iran

Accepted author version posted online: 12 May 2014.Published online: 02 Jun 2014.

To cite this article: Azam Zamani, Mehdi Salehi, S. Maryam Sajjadi, Maciej Kubicki, Grzegorz Dutkiewicz & Ali Khaleghian (2014) Synthesis, characterization, spectrophotometric investigation, structural study, and antibacterial activities of a series of new zinc(II) complexes, Journal of Coordination Chemistry, 67:10, 1782-1793, DOI: 10.1080/00958972.2014.921288

To link to this article: http://dx.doi.org/10.1080/00958972.2014.921288

Journal of Coordination Chemistry, 2014
Vol. 67, No. 10, 1782–1793, http://dx.doi.org/10.1080/00958972.2014.921288

Synthesis, characterization, spectrophotometric investigation, structural study, and antibacterial activities of a series of new zinc(II) complexes

AZAM ZAMANI†, MEHDI SALEHI*†, S. MARYAM SAJJADI†, MACIEJ KUBICKI‡, GRZEGORZ DUTKIEWICZ‡ and ALI KHALEGHIAN§

†Department of Chemistry, College of Science, Semnan University, Semnan, Iran
‡Faculty of Chemistry, Adam Mickiewicz University, Poznan, Poland
§Department of Biochemistry, Semnan University of Medical Science, Semnan, Iran

(*Received 8 January 2014; accepted 21 March 2014*)

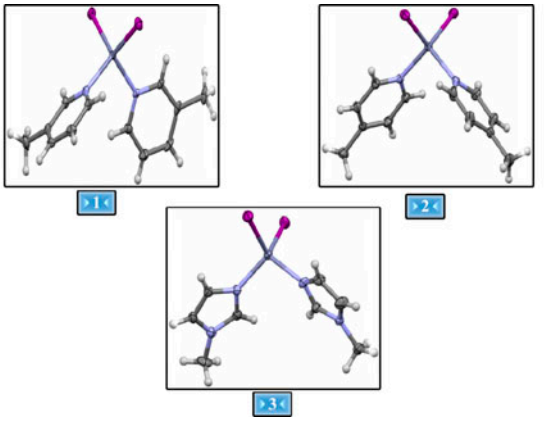

Three new zinc(II) complexes were investigated. These complexes were characterized by Fourier transform infrared (FT-IR), ^{1}H NMR and UV–vis spectroscopy. The crystal structures were determined by X-ray diffraction. The equilibrium formation constants of the complexes and the molar absorptivity profiles of the species were obtained by multivariate hard modeling analysis of UV–vis absorption spectral data. Also, biological activities of new compounds studied and good results obtained.

Tetrahedral [Zn(Amine)$_2$I$_2$] complexes which Amine = 3-methylpyridine (3-Mepy) (**1**), 4-methylpyridine (4-Mepy) (**2**), and *N*-methylimidazole (*N*-MeIm) (**3**) were synthesized and characterized by Fourier transform infrared, ^{1}H NMR, and UV–vis spectroscopy. The crystal structures of **1–3** were determined by X-ray diffraction and have distorted tetrahedral geometry. The equilibrium formation constants and the molar absorptivity profiles of the complexes were obtained by multivariate hard modeling analysis of UV–vis absorption spectral data. Biological activities of the complexes were also studied on *Staphylococcus aureus*, *Salmonella Typhi*, *Escherichia coli*, and *Bacillus subtilis* by the well diffusion method.

*Corresponding author. Email: msalehi@sun.semnan.ac.ir

Keywords: Antibacterial activities; Crystal structure; Model complex; Spectrophotometric investigation; Zinc(II) complexes

1. Introduction

Zinc is an essential element playing numerous roles in organisms. It is involved in the synthesis of proteins and DNA [1], because zinc stabilizes the structure of chromatin and affects the replication of DNA and transcription of RNA by regulating the activity of transcription factors of RNA and DNA polymerases [2]. Zinc is recognized as essential for the activity of a wide range of enzymes, including metalloenzymes such as zinc-peptidases [3], human carbonic anhydrase [4], alkaline phosphatase [5], and is also involved in enzymatic and catalytic processes [6, 7]. Zinc is closely connected with the generation of insulin, because zinc complexes could be used in treatment of diabetes [8, 9]. The lack of zinc causes health problems and disorders of the central nervous system, so there is an urgent demand for development of Zn^{2+}-specific molecular probes, exhibiting high selectivity and sensitivity over other biologically necessary metal ions in specific concentration ranges [10–12]. Diverse zinc(II) complexes have been studied in their biological activities, including antidiabetic [13], anticancer [14], anticonvulsant [15], anti-inflammatory [16], and antimicrobial [17] activities. Because of the d^{10} electronic configuration, it is not subjected to ligand field stabilization effects. Coordination number and geometry are therefore dictated only by ligand size and charge. This means that zinc can adopt highly flexible coordination geometries. However, in most zinc(II) complexes there is a strong preference for tetrahedral coordination, frequently slightly distorted, which enhances the Lewis acidity of the zinc center. Herein, we report the synthesis, spectroscopic characterization, and structural study of $[Zn^{II}(3\text{-Mepy})_2I_2]$ (**1**), $[Zn^{II}(4\text{-Mepy})_2I_2]$ (**2**), and $[Zn^{II}(N\text{-MeIm})_2I_2]$ (**3**) complexes (scheme 1). The formation constants of the complexes play an important role in interpretation of systems. Most of the methods of calculating these constants include the fitting of data to a physicochemical model or a mathematical equation [18–22]; these are called hard modeling methods. Here, one of the equilibrium systems, $[Zn^{II}(4\text{-Mepy})_2I_2]$, is monitored spectrophotometrically and the formation constants of the complex are calculated by the multivariate hard modeling method. In the present study for the first time, antibacterial activities of zinc(II) complexes against *Bacillus subtilis* (Gram-positive), *Staphylococcus aureus* (Gram-positive), *Salmonella Typhi* (Gram-negative), and *Escherichia coli* (Gram-negative) are investigated.

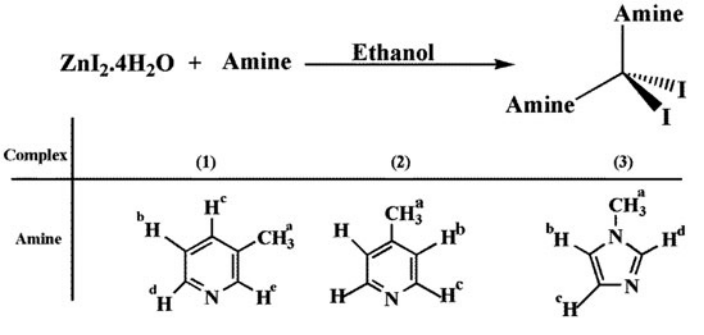

Scheme 1. Formation of **1**, **2**, and **3**.

2. Experimental

2.1. *Reagents and measurements*

All solvents and chemicals were used as received. ^{1}H NMR spectra were obtained on a BRUKER AVANCE DR X300 (300 MHz) spectrometer using $CDCl_3$ as solvent. IR spectra were recorded on a Bruker FT-IR instrument using KBr plates. UV–vis spectra were also obtained on a Shimadzu UV-1650PC spectrophotometer.

2.2. *Synthesis and characterization*

2.2.1. Synthesis of $[Zn^{II}(3\text{-Mepy})_2I_2]$ (1). 3-Mepy (0.09 mL, 1 mM) was added to $ZnI_2{\cdot}4H_2O$ (0.159 g, 0.5 mM) in methanol (10 mL), and the resultant colorless reaction mixture was stirred at room temperature for 1 h to give a clear solution. Colorless single crystals were obtained by slow evaporation of the solution in air. The yield of the reaction was 50%. IR (KBr, cm^{-1}): 1609 (C=C), 1600 (C=N), 410 (Zn–N). UV–vis: λ_{max} (nm), ε ($L\,M^{-1}\,cm^{-1}$) (CH_3CN) 212 (25,000), 264 (6000). ^{1}H NMR (300 MHz, ($CDCl_3$, δ, ppm): 2.32 (t, $3H_a$), 7.16 (s, H_b), 7.45 (dd, H_c), 7.75 (d, H_d), 8.55 (m, H_e).

2.2.2. Synthesis of $[Zn^{II}(4\text{-Mepy})_2I_2]$ (2). This complex was prepared by the same method as for **1** except that 4-MePy was used instead of 3-MePy. Colorless crystals of **2** suitable for X-ray crystallography were obtained after three days by slow evaporation of the solvent. The crystals were filtered off and washed with a small amount of cold methanol and dried under vacuum. The yield of the reaction was 65%. IR (KBr, cm^{-1}): 1625 (C=C), 1616 (C=N), 489 (Zn–N). UV–vis: λ_{max} (nm), ε ($L\,M^{-1}\,cm^{-1}$) (CH_3CN) 212 (23,000), 250 (6000). ^{1}H NMR (300 MHz, ($CDCl_3$, δ, ppm): 2.34 (t, $3H_a$), 7.40 (d, $2H_b$), 8.62 (d, $2H_c$).

2.2.3. Synthesis of $[Zn^{II}(N\text{-MeIm})_2I_2]$ (3). This complex was synthesized by the same method as for **1** except that *N*-MeIm was used instead of 3-MePy. A colorless microcrystalline solid was produced by slow evaporation of methanol at room temperature. The product was then recrystallized from methanol and colorless crystals suitable for X-ray crystallography were obtained. The crystals were filtered off and washed with a small amount of cold methanol and dried under vacuum. The yield of the reaction was 45%. IR (KBr, cm^{-1}): 1610 (C=C), 1596 (C=N), 440 (Zn–N). UV–vis: λ_{max} (nm), ε ($L\,M^{-1}\,cm^{-1}$) (CH_3CN) 214 (27,000), 248 (4000).^{1}H NMR (300 MHz, ($CDCl_3$, δ, ppm): 3.64 (t, $3H_a$), 6.86 (s, H_b), 7.38 (d, H_c), 8 (s, H_d).

2.3. *X-ray crystallography*

Diffraction data were collected at room temperature (**1** and **2**) and at 100(1) K (**3**) by the ω-scan technique on an Agilent Technologies Xcalibur four-circle diffractometer with Eos CCD-detector and graphite-monochromated Mo K_α radiation ($\lambda = 0.71073$ Å). The data were corrected for Lorentz-polarization as well as for absorption effects [23]. Precise unit-cell parameters were determined by a least-squares fit of 3823 (**1**), 7634 (**2**), and 3361 (**3**) reflections of highest intensity. The structures were solved by SIR92 [24] and refined with full-matrix least-squares on F^2 by SHELXL97 [25]. The scattering factors incorporated in

SHELXL97 were used. The function $\sum w(|F_o|^2 - |F_c|^2)^2$ was minimized, with $w^{-1} = [\sigma^2(F_o)^2 + (A \cdot P)^2 + B \cdot P]$ ($P = [\text{Max}\ (F^2_o, 0) + 2F^2_c]/3$). The final values of A and B are listed in table 1. All non-hydrogen atoms were refined anisotropically; hydrogens were placed geometrically in idealized positions and refined as rigid groups with their U_{iso}'s as 1.2 or 1.5 (methyl) times U_{eq} of the appropriate carrier atom. Relevant crystal data are reported in table 1 together with refinement detail.

2.4. *Spectrophotometric investigation of $[Zn^{II}(4\text{-MePy})_2I_2]$ as a case study*

We were interested in the spectrophotometric investigation of one complex as a case study. In an experiment, 1.5 mL of $ZnI_2 \cdot 4H_2O$ solution in methanol (0.14 M) was transferred to a cuvette. The UV–vis spectrum was recorded in the wavelength range of 290–490 nm with 1 nm increment, about 5 min after each addition of 10 µL of 4-MePy (3.1 M) in methanol solution (figure 1).

2.5. *Antibacterial assay*

The zinc(II) complexes were screened *in vitro* for their antibacterial activity against two Gram-positive (*B. subtilis*; PTCC No: 1023; ATCC 6633 and *S. aureus*; PTCC No: 1431; ATCC 25,923) and Gram-negative (*S. Typhi*; PTCC No: 1175; ATCC 19,430 and *E. coli*; PTCC No: 1399; ATCC 25,922). Minimum inhibitory concentrations (MICs) were determined by the broth twofold dilution method as a quantitative assay [26]. Briefly, serial diluted chemical compounds of 0.01–0.52 mg mL^{-1} were added to final inoculums of approximately 1.5×10^6 organisms per mL in log phase growth. The cultures were

Table 1. Crystal data, data collection and structure refinement.

Compound	**1**	**2**	**3**
Formula	$C_{12}H_{14}I_2N_2Zn$	$C_{12}H_{14}I_2N_2Zn$	$C_8H_{12}I_2N_4Zn$
Formula weight	505.42	505.42	483.39
Crystal system	Monoclinic	Monoclinic	Orthorhombic
Space group	$P2_1/n$	$P2_1/c$	Pbca
a (Å)	9.401(2)	16.171(3)	14.483(3)
b (Å)	15.010(3)	14.648(3)	12.914(2)
c (Å)	11.115(2)	14.918(2)	15.004(3)
β (°)	99.29(1)	117.44(3)	90
V (Å^3)	1547.9(5)	3136.2(13)	2806.2(9)
Z	4	8	8
Dx (gcm^{-3})	2.169	2.141	2.288
F (0 0 0)	944	1888	1792
μ (mm^{-1})	5.557	5.486	6.129
θ Range (°)	3.0–28.2	2.9–28.2	3.0–28.2
hkl_{max}	12,19,13	21,19,19	18,16,19
Reflections			
Collected	6254	13,022	7649
Unique (R_{int})	3209(0.021)	6528(0.019)	2953(0.033)
With $I > 2\sigma(I)$	2903	5822	2662
Number of parameters	155	312	138
Weighting scheme			
A	0.0201	0.0165	0.0827
B	0.1338	0.4434	7.8969
R index [All data]	$R_1 = 0.023$; $wR_2 = 0.043$	$R_1 = 0.026$; $wR_2 = 0.045$	$R_1 = 0.048$; $wR_2 = 0.129$
Goodness-of-fit on F^2	1.128	1.077	1.097
Max/min $\Delta\rho$ (e Å^{-3})	0.47/−0.77	0.49/−0.43	2.58/−1.610

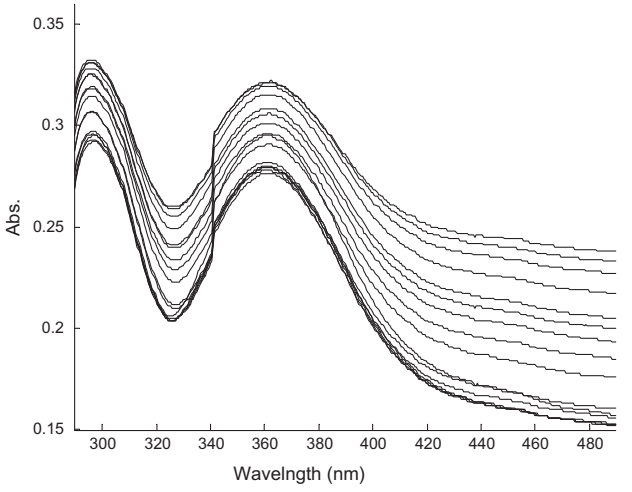

Figure 1. Titration absorption spectra of $ZnI_2 \cdot 4H_2O$ (0.14 M) with 4-Mepy.

incubated on a rotary shaker at 37 °C for 24 h. MIC ($\mu g\,mL^{-1}$) of each tested compound were defined as the lowest concentration exhibiting no visible growth compared with the drug-free control wells. Each organism was tested in duplicate on different days to measure the reproducibility of the test. To measure the minimal bactericidal concentration (MBC), 100 µL volumes of all clear (no growth) tubes from a dilution MIC test was spread on to separate agar plates and incubated at 37 °C for 24 h. The MBC ($mg\,mL^{-1}$) was defined as the lowest concentration of the complex that no growth occurred.

3. Results and discussion

3.1. *Synthesis*

The complexes, obtained by reaction of the aromatic amines with zinc iodide in methanol, were stable at room temperature and soluble in common polar organic solvents, such as dimethyl sulfoxide, dimethylformamide (DMF), methanol, ethanol, and acetonitrile.

3.2. *Infrared spectral study*

The solid state FT-IR spectra of the complexes showed a strong absorption band at 1600, 1616, and 1596 cm^{-1}, corresponding to the C=N stretch of **1**, **2**, and **3**, respectively. Another stretching vibration at 1609, 1625, and 1610 cm^{-1} was attributed to the C=C stretch of **1**, **2**, and **3**, respectively. Other low intensity bands in the range 400–500 cm^{-1} were assigned to Zn–N stretching vibrations.

3.3. *Electronic spectroscopy study*

Electronic absorption spectra of the complexes in acetonitrile showed intense absorptions from 200 to 270 nm, involving π–π^* transitions [26]. The band at lower wavelengths correspond to π–π^* transitions of the aromatic C=N bond, while the band at higher wavelengths was attributed to the π–π^* transitions of the aromatic C=C bond.

3.4. *^{1}H NMR spectral study*

^{1}H NMR spectral data of the complexes were obtained in $CDCl_3$, with chemical shifts expressed in ppm downfield from tetramethylsilane. In the Experimental section, the signals produced by ^{1}H NMR are reported. The signals corresponding to the aromatic protons of the amine rings were assigned as a singlet at 7.16 ppm (H_b), a doublet of doublets at 7.45 ppm (H_c), a doublet at 7.75 ppm (H_d), and a multiplet at 8.55 (H_e) ppm in **1**, two doublets at 7.40 ppm ($2H_b$) and 8.62 ($2H_c$) ppm in **2**, and two singlets at 6.86 ppm (H_b) and 8 (H_d) ppm and a doublet at 7.38 ppm (H_c) ppm in **3**. The signals due to the aliphatic protons of amine rings were observed as a triplet at 2.32 ppm ($3H_a$) in **1**, a triplet at 2.34 ppm ($3H_a$) in **2**, and a triplet at 3.64 ppm (H_a) in **3**. The structural integrity of these complexes in solution was confirmed by their ^{1}H NMR spectra in $CDCl_3$.

3.5. *Crystal structures*

The molecular structures of the complexes are shown in figures 2–4. Selected bond lengths and angles are listed in table 2. The complexes are structurally similar with Zn(II) in a pseudo-tetrahedral coordination geometry surrounded by two N-donors and iodides. The zinc(II) is coordinated by two amines and two iodides in a slightly distorted tetrahedral geometry. There are two crystallographically independent molecules in the asymmetric unit of **2**, but these molecules are chemically identical and geometrically very similar, showing some differences in their environments. The dihedral angles formed by the planes of the amine ligands are 82.19(8)°, 88.7(1)°, 79.9(1)°, and 61.33(2)° in **1**, **2A**, **2B**, and **3**, respectively. The tetrahedral geometry around zinc(II) in **1**, **2**, and **3** is distorted with different bond distances and angles. As expected, the deviation from ideal tetrahedral geometry is more significant for **1** than **2**, substantiated from the N–Zn–N, I–Zn–I, and I–Zn–N angles in table 2. Relatively weak C–H···I contacts (H···I distances 3.03–3.15 Å) as well as C–H···π interactions are to some extent involved in the crystal packing. These interactions in **3** are shown in figure 5.

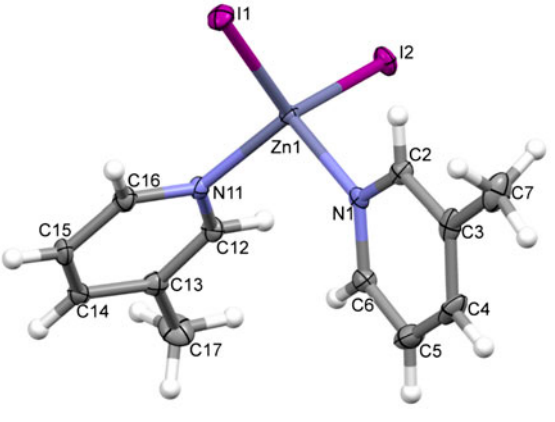

Figure 2. Perspective view of **1**; the ellipsoids are drawn at the 50% probability level, hydrogens are shown as spheres of arbitrary radii.

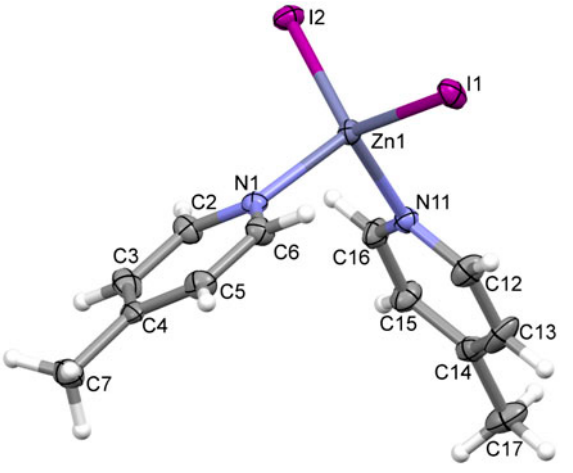

Figure 3. Perspective view of **2A**; the ellipsoids are drawn at the 50% probability level, hydrogens are shown as spheres of arbitrary radii.

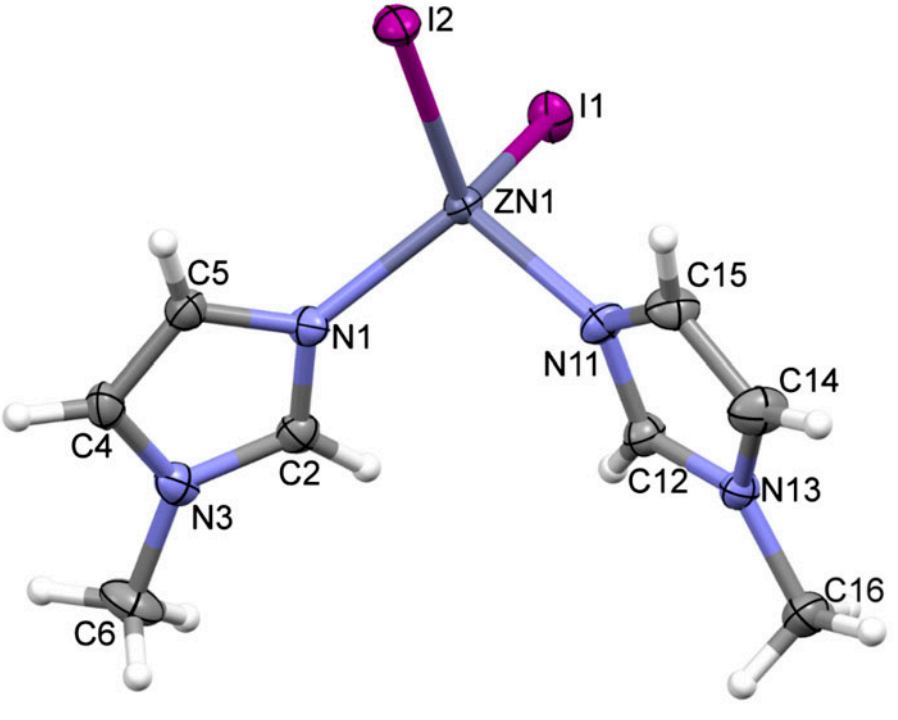

Figure 4. Perspective view of **3**; the ellipsoids are drawn at the 50% probability level, hydrogens are shown as spheres of arbitrary radii.

Table 2. Relevant geometrical parameters (Å, °) with su's in parentheses.

	1	2A	2B	3
Zn1–N1	2.048(2)	2.056(2)	2.050(2)	2.018(5)
Zn1–N11	2.052(2)	2.056(3)	2.067(3)	2.023(5)
Zn1–I1	2.5442(6)	2.5667(4)	2.5592(4)	2.5699(9)
Zn1–I2	2.5562(6)	2.5476(4)	2.5521(4)	2.5747(8)
N1–Zn1–N11	103.94(9)	101.35(9)	99.59(9)	104.1(2)
N1–Zn1–I1	106.09(6)	106.19(6)	106.42(6)	108.07(13)
N1–Zn1–I2	106.45(6)	110.91(6)	112.18(6)	110.29(14)
N11–Zn1–I1	109.15(6)	101.35(9)	108.18(6)	110.27(13)
N11–Zn1–I2	107.53(6)	106.47(6)	106.58(6)	109.19(13)
I1–Zn1–I2	122.213(13)	120.78(3)	121.620(15)	114.42(3)

3.6. *Spectral data analysis of the [Zn^{II}(4-MePy)$_2I_2$] complex by multivariate hard modeling method*

The titration spectrum of $ZnI_2{\cdot}4H_2O$ upon increasing addition of 4-Mepy is shown in figure 1. This titration consists of a collection of spectra of a solution measured as a function of addition of 4-Mepy which influences the equilibrium under investigation. The collected absorption spectra can be arranged as a matrix, **D**, where each spectrum is stored as rows [25]. The matrix **D** has N columns and M rows where N is the number of wavelengths for which the spectra were recorded and M is the number of titration points. According to Beer–Lambert's law, this matrix can be described as elements of **C**, times a matrix, **E**, of molar absorption spectra.

$$\mathbf{D} = \mathbf{C} \times \mathbf{E} + \mathbf{R}$$

The matrix $\mathbf{C}(M \times P)$ contains the concentration profiles of P equilibrium species. The matrix $\mathbf{E}(P \times N)$ consists of the molar absorption spectra of P components. There are several multivariate analysis methods for decomposition of data matrix **D**. However, none of the decomposition is perfect and a matrix **R** of residuals (of the same dimensions as **D**) represents the difference between the measurement, **D**, and its representation, $\mathbf{C} \times \mathbf{E}$. Instrumental noise and other experimental shortcomings such as errors in volumes, concentrations, impurities, etc. lead to matrix **R**. The goals of the analysis are calculating the equilibrium constant of [Zn^{II}(4-Mepy)$_2I_2$] and obtaining pure spectra of the complex. So, the matrix **D** should be decomposed into matrices **C** and **E**. There are several very different approaches to this end. A suitable method to achieve these purposes is multivariate hard modeling. This is based on a least-squares algorithm, which calculates the best set of parameters defined by a model. The parameters have to be set independently. In this method, the sum of squares is a function of a chemical model and its parameters:

$$\text{ssq} = \sum_{i=1}^{i=M} \sum_{j=1}^{j=N} (\mathbf{R}_{i,j}^2) = f(\mathbf{D}, \text{ Model, Parameters})$$

The best set of the parameters results in minimum ssq [25].

There are two types of parameters, linear and non-linear. For a given equilibrium model, the concentration matrix **C** is a function of equilibrium constants as nonlinear parameters. The molar absorptivity of all reacting species, which are the elements of matrix **E**, are linear parameters. What is interesting is that these linear parameters can effectively be eliminated

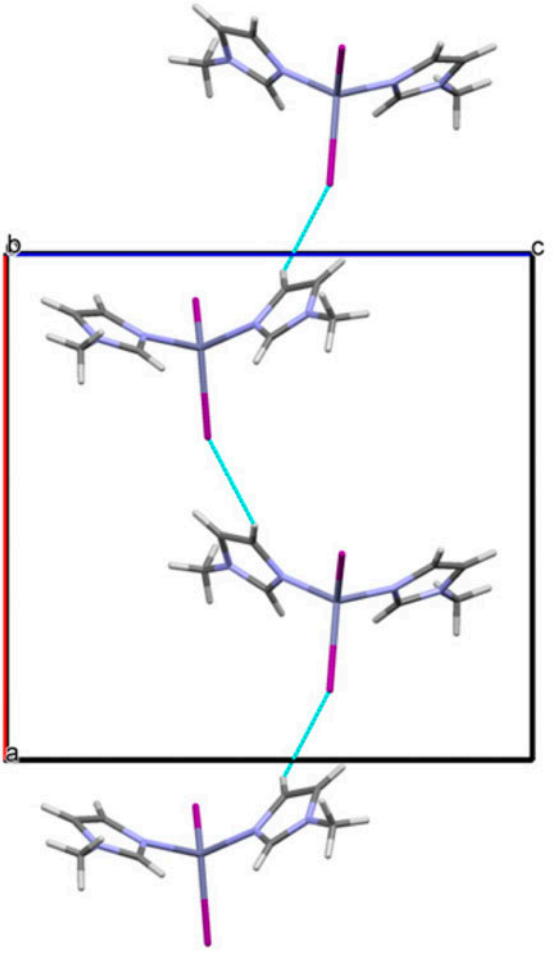

Figure 5. A fragment of a chain of the molecules **3** joined by the C–H···I interactions.

from the iterative process [26]. Thus, for a given model, the sum of squares can be defined as a function of only the non-linear parameter equilibrium constants and these parameters, which define **C**, are the only ones that need to be fitted in an iterative process. What makes the hard modeling method robust is the very small number of parameters. In this work, fminsearch function in Matlab, which is based on Nelder–Mead algorithm [27], was used for iterative non-linear fitting. During the optimization, Newton–Raphson algorithm calculates the concentration profiles of species. The volumes of starting metal solution and of added 4-MePy, total concentrations of Zn and 4-MePy components were needed to run the Newton–Raphson algorithm. Molar absorptivity spectra of metal and ligand were considered known parameters and the concentration and the molar absorptivity spectral profiles of $[Zn^{II}(4\text{-Mepy})(H_2O)I_2]$ and $[Zn^{II}(4\text{-Mepy})_2I_2]$, were obtained by applying the hard modeling method. The results of the analysis are shown in figures 6a and 6b. Benefits from hard modeling analysis are obtaining the molar absorptivity spectra of the intermediate $[Zn^{II}(4\text{-Mepy})(H_2O)I_2]$, which cannot be determined experimentally and computing the formation

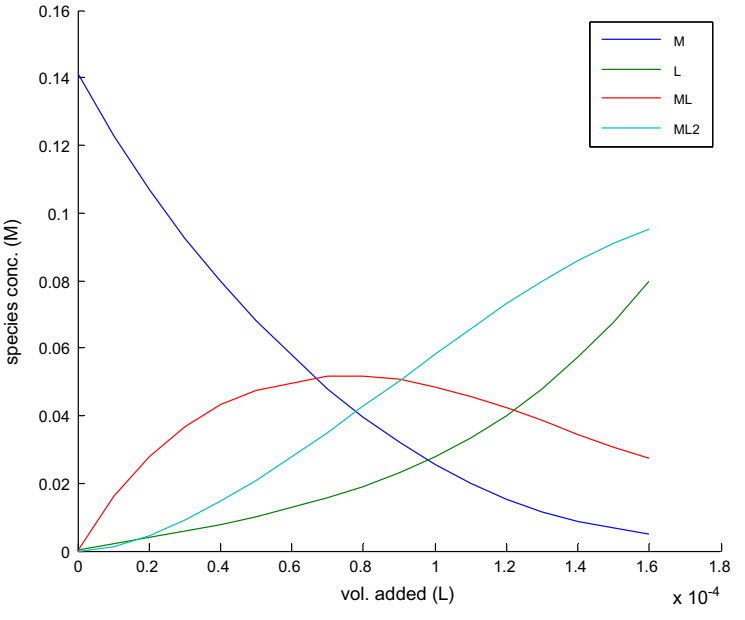

Figure 6a. Obtained concentration profiles by using hard modeling method; M and L denotes metal and ligand, respectively.

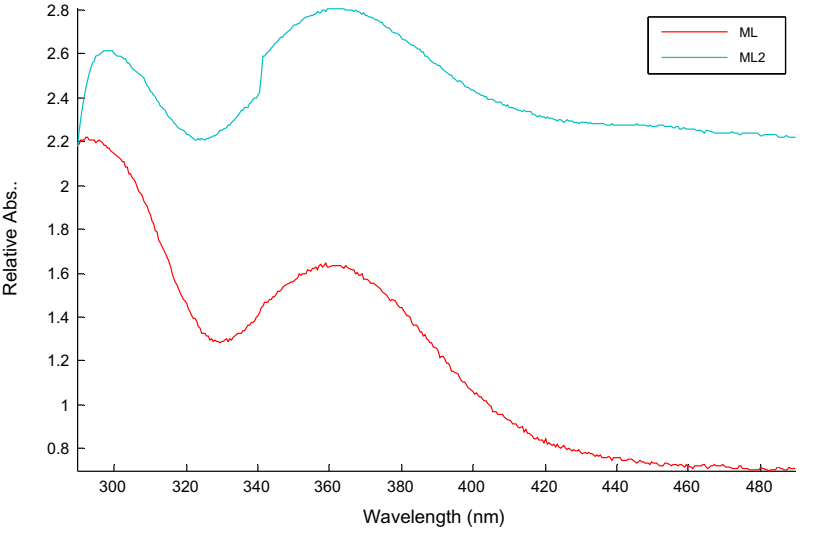

Figure 6b. Obtained molar absorptivity spectral profiles of two complexes by using hard modeling method; M and L denotes metal and ligand, respectively.

constants of the complex. The calculated formation constants of $[Zn^{II}(4\text{-Mepy})(H_2O)I_2]$ and $[Zn^{II}(4\text{-Mepy})_2I_2]$ are 6.9×10^1 and 3.0×10^3, respectively.

Table 3. MIC[a] of **1–3** against growth of bacteria ($\mu g\,mL^{-1}$).

Compound	*S. aureus*	*E. coli*	*B. subtilis*	*Salmonella Typhi*
1	175	1000	225	750
2	500	2500	750	2250
3	250	1250	500	1000
Kanamycin	3	3.8	3.6	3.2
Chloramphenicol	2.4	4.2	4	3.5

[a]MIC, minimal inhibitory concentration.

Table 4. MBC[a] of **1–3** against growth of bacteria ($\mu g\,mL^{-1}$).

Compound	*S. aureus*	*E. coli*	*B. subtilis*	*Salmonella Typhi*
1	225	1250	250	1000
2	750	2750	1000	2500
3	750	1500	750	1250
Kanamycin	3.2	4	3.6	3.3
Chloramphenicol	2.5	4.5	4	3.5

[a]MBC, minimal bactericidal concentration.

3.7. *Biological properties*

The *in vitro* antibacterial activity of **1–3** was evaluated against Gram-positive and Gram-negative bacteria. Kanamycin and chloramphenicol were used as references. The MICs and the MBC of the compounds against these bacteria are presented in tables 3 and 4. The results indicate that **1–3** were less active than standard drugs. Complexes **1** and **3** showed significant antibacterial activity against *B. subtilis* and *S. aureus* and moderate activity against *S. Typh* and *E. coli*. The activity of these complexes was compared with the zinc(II) complex of phenylthiourea [28]. The amine zinc(II) complexes showed higher activity because of the presence of more electron donating ligands present in these complexes. The variation in the effectiveness of various compounds against various organisms depends on the impermeability of the cells of the microbes [29].

4. Conclusion

We have prepared new zinc(II) complexes with amine and iodide ligands. The complexes have been characterized by various physical and chemical techniques. The crystal structures of **1**, **2** and **3** confirmed that they are mononuclear distorted tetrahedral complexes. The equilibrium system of $[Zn^{II}(4\text{-Mepy})_2I_2]$ was monitored spectrophotometrically. The formation constants of the complex and the molar absorptivity spectra of species are calculated by applying hard modeling method of spectrophotometric data. The complexes show relatively moderate activities against bacteria.

Supplementary material

CCDC 975470–975472 contains the supplementary crystallographic data for **1–3**. These data can be obtained free of charge from The Cambridge Crystallographic Data Center via www.ccdc.cam.ac.uk/data_request/cif.

Acknowledgement

We thank Semnan University for supporting this study.

References

[1] J.E. Cummings, J.P. Kovacic. *J. Vet. Emerg. Crit. Care*, **19**, 215 (2009).
[2] K.H. Falchuk. *Mol. Cell. Biochem.*, **188**, 41 (1998).
[3] (a) D.C. Rees, M. Lewis, W.N. Lipscomb. *J. Mol. Biol.*, **168**, 367 (1983); (b) D.R. Holland, A.C. Haustrath, D. Juers, B.W. Matthews. *Protein Sci.*, **4**, 1955 (1995).
[4] (a) S.K. Nair, D.W. Christianso. *J. Am. Chem. Soc.*, **113**, 9455 (1991); (b) D.N. Silverman, S. Lindskog. *Acc. Chem. Res.*, **21**, 30 (1988).
[5] E.E. Kim, H.W. Wyckoff. *J. Mol. Biol.*, **218**, 449 (1991).
[6] J.M. Berg, H.A. Godwin. *Annu. Rev. Biophys. Biomol. Struct.*, **26**, 357 (1997).
[7] (a) R. Puchta, B.M. Alzoubi, R. Meier, S.I. Almuhtaseb, M. Walther, R. van Eldik. *Dalton Trans.*, 14151 (2012); (b) A. Beck, B. Weibert, N. Burzlaff. *Eur. J. Inorg. Chem.*, **2001,** 521 (2001); (c) H. Vahrenkamp. *Acc. Chem. Res.*, **32**, 589 (1999); (d) M. Braüer, E. Anders, S. Sinnecker, W. Koch, M. Rombach, H. Brombacher, H. Vahrenkamp. *J. Chem. Soc., Chem. Commun.*, 647 (2000); (e) M. Tesmer, M. Shu, H. Vahrenkamp. *Inorg. Chem.*, **40**, 4022 (2001); (f) G.P.M. Stenta, D. Spinelli, E. Anders, A. Bottoni. *Theor. Chem. Acc.*, **118**, 193 (2007).
[8] P.D. Zalewski, S.H. Millard, I.J. Forbes, O. Kapaniris, A. Slavotinek, W.H. Betts, A.D. Ward, S.F. Lincoln, I. Mahadevan. *J. Histochem. Cytochem.*, **42**, 877 (1994).
[9] S. Fujimoto, H. Yasui, Y. Yoshikawa. *J. Inorg. Biochem.*, **121**, 10 (2013).
[10] T. Atsushi, T. Haruna. *Brain Res. Rev.*, **62**, 33 (2009).
[11] C.J. Chang, E.M. Nolan, J. Jaworski, S.C. Burdette, M. Sheng, S.J. Lippard. *Chem. Biol.*, **11**, 203 (2004).
[12] A. Ajayaghosh, P. Carol, S. Sreejith. *J. Am. Chem. Soc.*, **127**, 14962 (2005).
[13] H. Sakurai, Y. Kojima, Y. Yoshikawa, K. Kawabe, H. Yasui. *Coord. Chem. Rev.*, **226**, 187 (2002).
[14] J.S. Casas, E.E. Castellano, M.D. Couce, J. Ellena, A. Sanchez, J. Sordo, C. Taboada. *J. Inorg. Biochem.*, **100**, 124 (2006).
[15] J. d'Angelo, G. Morgant, N.E. Ghermani, D. Desmaele, B. Fraisse, F. Bonhomme, E. Dichi, M. Sghaier, Y. Li, Y. Journaux, J.R.J. Sorenson. *Polyhedron*, **27**, 537 (2008).
[16] Q. Zhou, T.W. Hambley, B.J. Kennedy, P.A. Lay, P. Turner, B. Warwick, J.R. Biffin, H.L. Regtop. *Inorg. Chem.*, **39**, 3742 (2000).
[17] N.C. Kasuga, K. Sekino, M. Ishikawa, A. Honda, M. Yokoyama, S. Nakano, N. Shimada, C. Koumo, K. Nomiya. *J. Inorg. Biochem.*, **96**, 298 (2003).
[18] M. Maeder, A.D. Zuberbuhler. *Anal. Chem.*, **62**, 2220 (1990).
[19] A.D. Juan. *Chemometr. Intell. Lab. Syst.*, **54**, 123 (2000).
[20] S. Bijlsma, A.K. Smilde. *Anal. Chim. Acta*, **396**, 231 (1999).
[21] J. Inczedy. *Analytical Applications of Complex Equilibria*, Wiley, New York (1976).
[22] A.E. Martell, R.J. Motekaitis. *Determination and Use of Stability Constant*, 2nd Edn, V.C.H., Weinheim (1992).
[23] Agilent Technologies. *Crysalis PRO (Version 1.171.33.36d)*, Oxford Diffraction Ltd., Poznan (2010).
[24] A. Altomare, G. Cascarano, C. Giacovazzo, A. Gualardi. *J. Appl. Crystallogr.*, **26**, 343 (1993).
[25] G.M. Sheldrick. *Acta Cryst.*, **A64**, 112 (2008).
[26] EUCAST. *Clin. Microbiol. Infect.*, **6**, 509 (2000).
[27] J.R. Zamian, E.R. Dockal. *Transition Met. Chem.*, **21**, 370 (1996).
[28] P.A. Ajibade, N.H. Zulu. *J. Coord. Chem.*, **63**, 3229 (2010).
[29] T.D. Thangadurai, K. Natarajan. *Transition Met. Chem.*, **27**, 485 (2002).